Frequency Effects on Sonoluminescence of Alkali-Metal Atoms in Sulfuric Acid

Shin-ichi Hatanaka (1), Shigeo Hayashi (1) and Pak-Kon Choi (2)

(1) The University of Electro-Communications, 1-5-1 Chofugaoka, Chofu, Tokyo 182-8585 Japan
(2) Meiji University, 1-1-1 Higashimita, Tama-ku, Kawasaki, Kanagawa, 214-8571 Japan

PACS: 43.25.YW

ABSTRACT

Intense orange Na* emission was observed in different spatial locations from blue emission during multibubble sonoluminescence in sulfuric acid. The color change from blue to orange was observed along the streamer in the filamentous structure of a bubble cloud. By stroboscopic observation, the Na* emission seemed to occur when a large bubble ejected tiny bubbles at the positions toward a pressure node after bubble coalescence around a pressure antinode. The intensity of Na* emission in the sulfuric acid increased at lower frequency in contrast with that in water. By comparing a high-resolution Na* spectrum of sulfuric acid with that of water, the widths of the spectra were almost the same, except for something being superimposed in the water case. The estimations of the temperature and pressure inside the Na* emission bubbles at 28 and 150 kHz were 1900 K and 100 atm and 2200 K and 150 atm, respectively.

INTRODUCTION

Recently, extremely intense sonoluminescence in sulfuric acid has been discovered in both single bubble sonoluminescence (SBSL) [1-2] and multibubble sonoluminescence (MBSL) [3], which is 1500 times brighter than previous sonoluminescence in water. In sulfuric acid, new emission lines of noble gas atom emission and molecular (SO) and ionic (O^{2+}) emissions were also observed. These studies have given many experimental lines of evidence of theoretical studies and have continued to provide further insight into the physical conditions and chemical processes occurring during SBSL and MBSL [4-14].

One of the most important discoveries of sonoluminescence in sulfuric acid for sonochemistry is the emission from electronically excited metal atoms during SBSL [7] and MBSL [14]. Flannigan and Suslick [7] has provided further insight into how nonvolatile metal cations become heated in a collapsing bubble. In that paper, the observations supported the hypothesis that nonvolatile species can only enter the bubble when the macroscopic bubble motion becomes sufficiently chaotic for energetic surface oscillations to develop and thus entrain liquid droplets in the bubble interior (illustrated as an injected droplet model [7]).

Alkali-metal atom emissions during MBSL are becoming more important in sonochemistry, because Sunartio et al. have suggested that Na* emission arises from sonochemically active bubbles that are not producing sonoluminescence [15]. The temperature and pressure inside the bubbles that emit alkali-metal emissions were reported by Sehgal et al. [16], but doubted by Flint and Suslick [17]. Although there are many papers concerning the emission from excited alkali-metal atoms observed during MBSL [15-20], the physics and chemistry are still not well understood.

In this study, we have examined alkali-metal emissions during MBSL in sulfuric acid with sodium sulfate, in comparison with those in aqueous solutions. The present study may provide further insight into the origin of alkali-metal emissions, because the extremely intense emission of excited sodium atoms, as well as the intense continuum, can be observed separately. Moreover, the bubble dynamics is relatively slow in the translational motion of bubbles due to the higher viscosity of sulfuric acid than that of water.
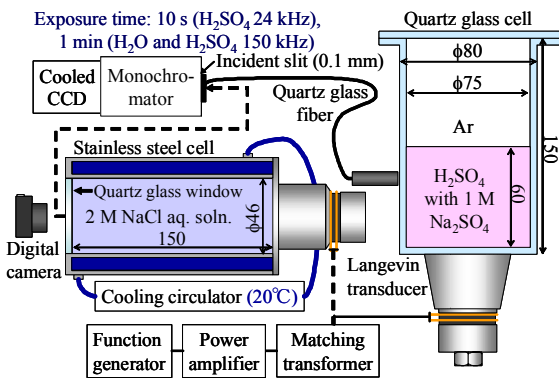
EXPERIMENT

The sulfuric acid (H_2SO_4) used was of ultrapure grade (purity: 97.0-98.0%) and sodium sulfate (Na_2SO_4) and sodium chloride were of special pure grade (min. 99.0%). They were purchased from Kanto Chemical Co. Inc., Japan and used as received. H_2SO_4 into which Na_2SO_4 powder was added was degassed under vacuum with stirring and then left under Xe or Ar gas atmosphere for a sufficient time to dissolve the gases. The Na_2SO_4 concentration in sulfuric acid was 1 mol/L, whereas the concentration of NaCl aqueous solution was 2 mol/L; the concentration of the Na+ cation was the same in both the sulfuric acid and aqueous solutions.

The experimental setup is shown in Fig. 1. Two different experimental apparatus and three different cells were used. Figure 1(a) shows the experimental setup for the simultaneous measurement of MBSL spectra and stroboscopic observation of cavitation bubbles in 1 M sodium sulfate sulfuric acid solution under Xe, which will correspond to the results in Figs. 2-4. Figure 1(b) shows the experimental setup for the comparison of the high-resolution spectra of MBSL under Ar in sulfuric acid solution with those in aqueous solution, which will correspond to the results in Figs. 5-10.
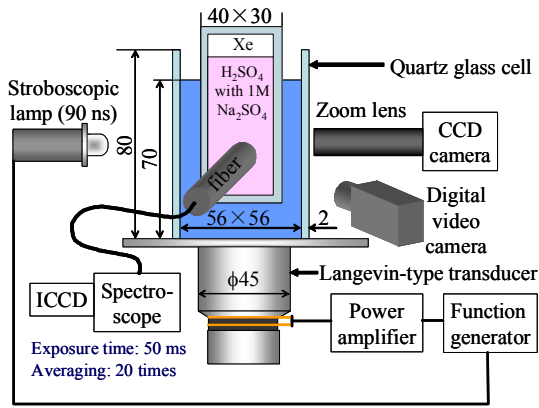
Figure 1. Experimental setups (a) for simultaneous measurement of MBSL spectra and stroboscopic observation of cavitation bubbles, and (b) for comparison between MBSL in sulfuric acid and aqueous solutions.

In Fig. 1(a), a continuous sinusoidal signal generated with a function generator (NF WF1946) was amplified with a power amplifier (Yokogawa 7058-10), and then applied to a Langevin-type transducer (Honda Electronics, resonance frequencies: 23, 44, and 95 kHz). The transducer was attached to a stainless steel plate, which is the bottom plate of a quartz glass cell of $56 \times 56 \times 80$ mm^3 inner size. In the cell, degassed distilled water was added and another quartz glass cell of $40 \times 30 \times 80$ mm^3 size was set in the water. A solution of 1 M Na_2SO_4-H_2SO_4 was added to an appropriate volume to establish a planelike standing wave field in the cell, which was confirmed with a hydrophone. Movies of MBSL were captured with a digital video camera (Sony DCR-TRV50). The spectrum of MBSL was obtained with a quartz glass fiber with 50 ms exposure and 20 times averaging using a spectroscope (Hamamatsu C8801-01), the detector of which was an intensified charge coupled device (ICCD). The behavior of cavitation bubbles was observed using a CCD camera with a backlight of stroboscopic flash pulse of 90 ns in full width at half maximum (FWHM). The method and instrumentation of the stroboscopic observation of cavitation bubbles are described in detail elsewhere [21-22].

In Fig. 1(b), two cylindrical cells made of different materials were used. A quartz glass cell and a stainless steel cell were used for the sulfuric acid solution and aqueous solution, respectively. The size of the quartz glass cell was $\phi75$ mm inner diameter $\times 150$ mm height. On the bottom of the cell, a Langevin-type transducer (Fuji Ceramics, resonance frequency: 28 kHz) was attached. The size of the stainless steel

cell, which was a coaxial cylinder, was $\phi46$ mm inner diameter $\times 150$ mm width. In the space between the inner cylinder and outer cylinder, cooling water of 20℃ was circulated with a cooling circulator. On one side of the cell, a Langevin-type transducer was attached, and a quartz glass window was placed on the opposite side. The cells used here are also described elsewhere [23-25]. A continuous sinusoidal signal generated with a function generator (NF WF1944A) and amplified with a power amplifier (E and I 1020L) was applied to the transducers through an impedance-matching transformer. The power amplifier showed both the forward and backward electrical outputs, and then the net electrical power input to the transducer was measured. Spectra of MBSL were collected using a system of a monochromator (Acton Research, SpectraPro-300i) and a cooled CCD detector (Princeton, Pixis). In the case of the sulfuric acid solution, MBSL spectra were collected through a quartz glass fiber with exposures of 10 s and 1 min for 24 and 150 kHz, respectively. In the case of the aqueous solution, MBSL spectra were collected with an exposure of 1 min without the fiber because of the lower intensity of MBSL; the quartz glass window of the cell closely faced the incident slit (0.1 mm) of the monochromator.

RESULTS AND DISCUSSION

Dynamics of Na* emission bubbles

Figure 2 shows two successive frames selected from a video recording of MBSL in 1 mol/L Na_2SO_4-H_2SO_4 solution under Xe at 44.5 kHz. The video frame rate is 15 frames per second (fps), which is half the conventional video frame rate of 30 fps (slow shutter mode). Orange emission is clearly seen in different spatial locations from blue-white emission. In the frame, a planelike standing wave field was established, where the position of a pressure node is around the center of the frame and the positions of pressure antinodes correspond to the blue-white emission regions. The distance between the blue-white emission regions is about 14 mm. In the video or in the observation with the naked eyes, a blue streamer seemed to move toward around the pressure antinodes, while an orange streamer seemed to move from the pressure antinodes toward the pressure node.
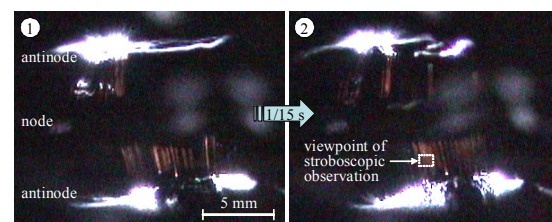

Figure 2. Two successive frames from a video at 15 fps for MBSL at 44.5 kHz in 1 M Na_2SO_4 sulfuric acid solution under Xe.
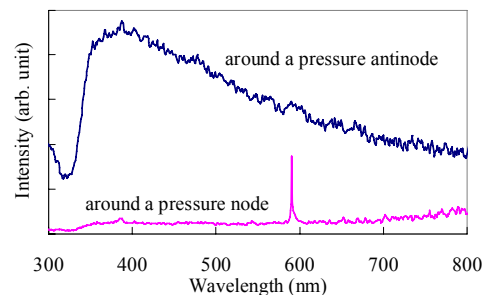

Figure 3. Corresponding MBSL spectra in the orange region below the pressure node and the blue-white one around the downside pressure antinode in Fig. 2.
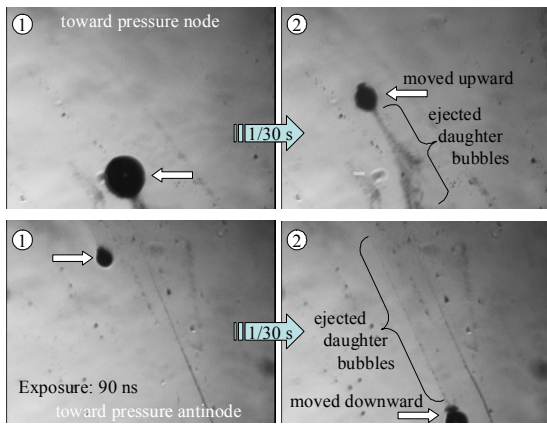
Figure 4. Two successive stroboscopic images of cavitation bubbles at 30 fps in the orange region below the pressure node in the field of view shown in Fig. 2.

Figure 3 shows spectra collected in the positions corresponding to the positions of the orange emission region below the pressure node and blue-white emission region around the downside pressure antinode in Fig. 2. It is confirmed that the sodium atom emission at 590 nm appears only in the orange emission region and is not included in the blue-white emission region, which agrees well with the colors of the frames in Fig. 2 and of the appearance observed with the naked eye.

Figure 4 shows the result of stroboscopic observation of cavitation bubbles in the orange emission region below the pressure node in Fig. 2, where the viewpoint of this stroboscopic observation is shown. Figure 4 shows selected sets of two successive frames at 30 fps that captured bubble entrainments, which consist of daughter bubbles ejected from a relatively large bubble. Since the stroboscopic flash light was the very short pulse of 90 ns in FWHM, the dark lines in the frames are bubble entrainments rather than bubble trajectories. It is seen that the large bubble recoiled from the ejected daughter bubbles and moved in the direction opposite to the ejection of the daughter bubbles. The top set of two frames shows that the large bubble moved upward toward the pressure node, while the bottom set of two frames shows that the large bubble moved downward toward the pressure antinode. In the downside blue-white emission region, it was observed that relatively large bubbles were produced by the coalescence of bubbles and moved upward toward the pressure node, although it was not shown here. Similar behaviors of bubble coalescence around a pressure antinode are photographed in detail elsewhere [26]. By comparing the distribution of the bubbles with that of the orange emission region, it seems that the line shape of the orange emission region corresponds to the daughter bubble entrainments. Na* emission may occur from the daughter bubbles when a large bubble ejects daughter bubbles, although there is no evidence of this yet.

Comparison of MBSL at 28 and 150 kHz

Figures 5 and 6 show the comparison of MBSL distribution under Ar between 28.0 and 150.0 kHz. Figure 5 shows the photographs in 1 M Na2SO4 sulfuric acid solution and Fig. 6 shows those in 2 M NaCl aqueous solution. In the case of the sulfuric acid, orange emission regions appear clearly in the different regions from blue-white emission ones at 28 kHz. In contrast, at 150 kHz in sulfuric acid, no orange emission can be seen in the photograph. On the other hand, in the case of the aqueous solution, the orange emission regions are dominant both at 28 and 150 kHz. It is possible that the difference can result from the difference in viscosity. The viscosity of sulfuric acid of 26.7 mPa·s (20℃) is much higher than that of water of 1.00 mPa·s (20℃). Moreover, the dynamics of cavi
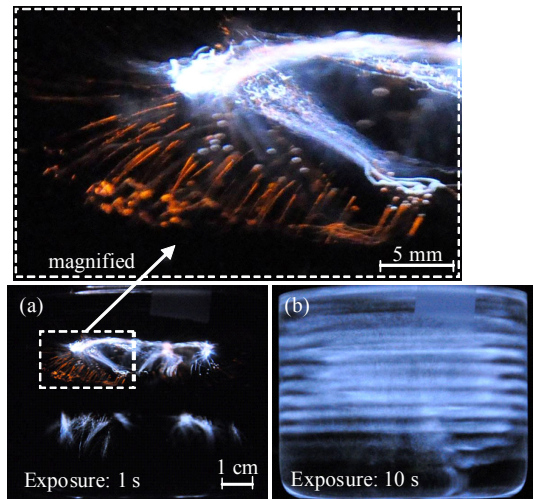

Figure 5. MBSL in 1 M Na$_2$SO$_4$ sulfuric acid solution under Ar at (a)28 and (b)150 kHz where the net power inputs to the transducer are 18 and 27 W, respectively.
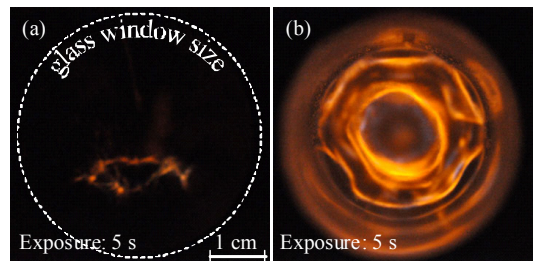

Figure 6. MBSL in 2 M NaCl aqueous solution under Ar at (a)28 and (b)150 kHz where the net power inputs to the transducer are 20 and 26 W, respectively.
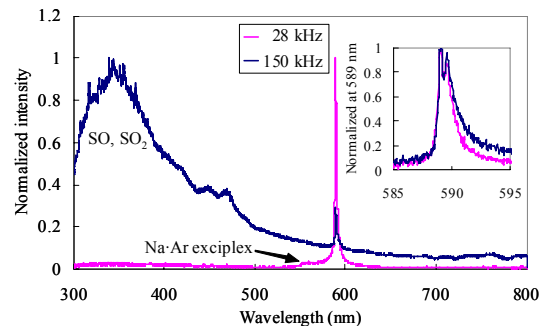

Figure 7. MBSL spectra in 1 M Na$_2$SO$_4$ sulfuric acid solution under Ar at 28 and 150 kHz corresponding to Fig. 5. Inset is the high-resolution spectra. The spectrum at 28 kHz is the one obtained when the optical fiber tip adjusted to the orange region.
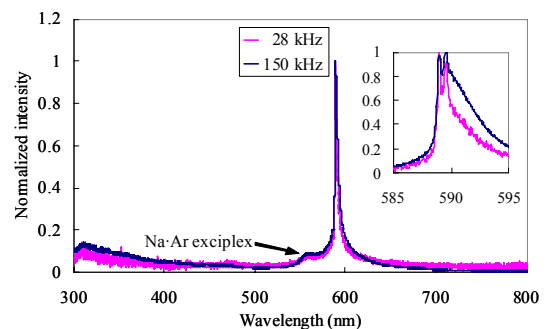

Figure 8. MBSL spectra in 2 M NaCl aqueous solution at 28 and 150 kHz corresponding to Fig. 6. Inset is the high-resolution spectra.

tation bubbles is known to be less violent at higher frequency. Therefore, assuming that Na* emission can occur from ejected daughter bubbles, at 150 kHz in sulfuric acid, bubbles could hardly eject daughter bubbles, as shown in Fig. 4, because of the high viscosity and high frequency, relative to the bubbles at 24 kHz in sulfuric acid and at 24 and 150 kHz in water.

Figures 7 and 8 show the MBSL spectra corresponding to Figs. 5 and 6, respectively. The spectra in each figure are normalized at maximum intensity. In the sulfuric acid case, as shown in Fig. 7, the spectrum at 150 kHz is different from that at 28 kHz. The spectrum at 150 kHz is mainly continuum, although there is a small sodium atom emission relative to the continuum. On the other hand, in the aqueous solution case, as shown in Fig. 8, the spectra at 28 and 150 kHz are almost the same.

Figures 9 and 10 show the comparison of a high-resolution Na* emission spectrum of sulfuric acid with that of water at 28 and 150 kHz, respectively. It is seen that the spectra are more tailing toward longer wavelengths in the aqueous solution than those in sulfuric acid. However, at 28 kHz, as shown in Fig. 9, the tailing starts at 0.6 in normalized intensity, which seems that another spectrum is superimposed. Apart from the superimposed spectrum, the widths of the sodium atom spectra are almost the same. In Fig. 10, the sodium atom spectrum in the aqueous solution is no longer separable, although the tailing seems abnormal. Thus, it is uncertain whether the width of the sodium atom spectrum in the aqueous solution is the same as that in sulfuric acid. However, it is possible that the widths of the sodium atom spectra are also the same at 150 kHz, similar to those at 28 kHz.

Sehgal et al. estimated the temperatures and pressures inside cavitation bubbles from the widths of sodium and potassium atom emissions during MBSL, which is historically the first estimation of cavitation temperature experimentally using sonoluminescence [16]. However, Flint and Suslick reported that the temperature probe of cavitation bubbles using alkali-metal atom emission is questionable, because the width of alkali-metal atom emission was independent of both the vapor pressures of the solvent and the species of the noble gases [17]. Then, instead of alkali metal atom emission, Suslick et al. reported cavitation temperatures using organic metal atom emission, given that organic metals are highly volatile [27]. However, our results show that the inaccuracy of widths of alkali-metal atom emission as the cavitation probe may result from some other spectrum superimposed on the alkali-metal atom emission. The widths of sodium atom emissions in sulfuric acid may be appropriate as the cavitation probe, because concentrated sulfuric acid has an extremely low vapor pressure, and decomposition product such as SO and SO_2 are highly soluble in sulfuric acid, whereas water has a higher vapor pressure than sulfuric acid and H_2 and O_2 are produced during ultrasonic irradiation of water under Ar.

Therefore, we estimated the temperatures and pressures inside cavitation bubbles from the full width at half maximum of sodium atom emissions in sulfuric acid. The estimation procedure was the same as that of Sehgal et al [16]. The half peak width of a sodium lamp was subtracted from the half peak width of sodium atom emission in MBSL to obtain the effect of only pressure broadening. By using the data on pressure broadening of emission spectra [28], it was possible to determine the relative densities of the emission phase of the cavity. By assuming that the mass of gas is constant during the collapse, the maximum temperature and pressure were determined from the adiabatic expression. The estimations of the temperatures and pressures inside the Na* emission
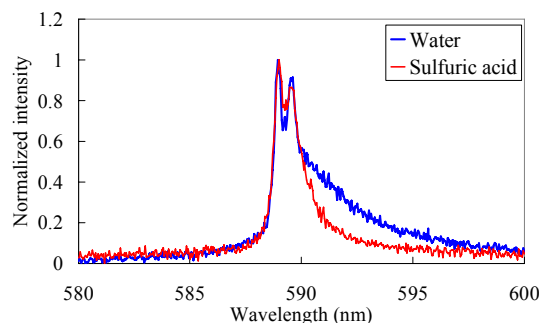

Figure 9. Comparison between high-resolution spectra of Na* emissions in sulfuric acid and aqueous solutions at 28 kHz.
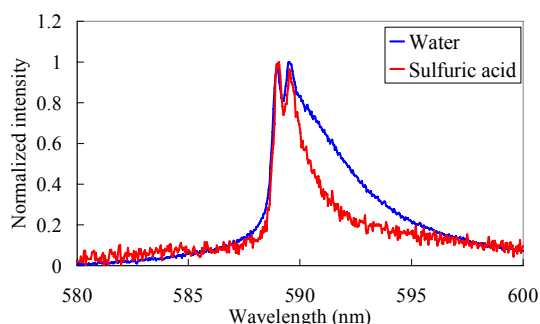

Figure 10. Comparison between high-resolution spectra of Na* emissions in sulfuric acid and aqueous solutions at 150 kHz.

bubbles at 28 and 150 kHz were 1900 K and 100 atm and 2200 K and 150 atm, respectively. Note that the temperatures are close to the temperature of the liquid phase (a possibility of liquid droplets within cavitation bubbles) reported by Suslick et al [29].

CONCLUSIONS

High-intensity sodium atom emission was observed in different spatial locations from blue emission during multibubble sonoluminescence in sulfuric acid. The color change from blue to orange was observed along the streamer in the filamentous structure of a bubble cloud. By stroboscopic observation, the sodium atom emission seemed to occur when a large bubble ejected tiny bubbles at the positions toward a pressure node after bubble coalescence around a pressure antinode. The intensity of sodium atom emission in the sulfuric acid case increased at the lower frequency of 28 kHz, whereas those in the aqueous solution case were almost the same at 28 and 150 kHz. By comparing a high-resolution sodium atom emission spectrum of sulfuric acid with of water, the full widths at half maximum of the spectra were almost the same, except for something being superimposed in the water case. The estimations of the temperature and pressure inside the sodium atom emission bubbles at 28 and 150 kHz were 1900 K and 100 atm and 2200 K and 150 atm, respectively.

ACKNOWLEDGEMENT

REFERENCES

1   D. J. Flannigan and K. S. Suslick, "Plasma formation and temperature measurement during single-bubble cavitation," *Nature* **434**, 52-55 (2005).

2   D. J. Flannigan and K. S. Suslick, "Plasma line emission during single-bubble cavitation," *Phys. Rev. Lett.* **95**, 044301 (2005).

3   N. C. Eddingsaas and K. S. Suslick, "Evidence for a plasma core during multibubble sonoluminescence in sulfuric acid," *J. Am. Chem. Soc.* **129**, 3838-3839 (2007).

4   S. D. Hopkins, S. J. Putterman, B. A. Kappus, K. S. Suslick, and C. G. Camara, "Dynamics of a sonoluminescing bubble in sulfuric acid," *Phys. Rev. Lett.* **95**, 254301 (2005).

5   G. L. Sharipov, A. M. Abdrakhmanov, and R. K. Gainetdinov, "Sonoluminescence of aqueous solutions of sulfuric acid and sulfur dioxide," *Russ. Chem. Bull.* **52**, 1966-1968 (2003).

6   D. J. Flannigan, S. D. Hopkins, C. G. Camara, S. J. Putterman, and K. S. Suslick, "Measurement of pressure and density inside a single sonoluminescing bubble," *Phys. Rev. Lett.* **96**, 204301 (2006).

7   D. J. Flannigan and K. S. Suslick, "Emission from electronically excited metal atoms during single-bubble sonoluminescence," *Phys. Rev. Lett.* **99**, 134301 (2007).

8   G. F. Puente, P. Garcia-Martinez, and F. J. Bonetto, "Single-bubble sonoluminescence in sulfuric acid and water: Bubble dynamics, stability, and continuous spectra," *Phys. Rev. E* **75**, 016314 (2007).

9   R. Urteaga and F. J. Bonetto, "Trapping an intensely bright, stable sonoluminescing bubble," *Phys. Rev. Lett.* **100**, 074302 (2008).

10 W. Z. Chen, W. Huang, Y. Liang, X. X. Gao, and W. C. Cui, "Time-resolved spectra of single-bubble sonoluminescence in sulfuric acid with a streak camera," *Phys. Rev. E* **78**, 035301 (2008).

11 J. S. Jeon, C. Lim, and H. Y. Kwak, "Measurement of pulse width of sonoluminescing gas bubble in sulfuric acid solution," *J. Phys. Soc. Jpn.* **77**, 033703 (2008).

12 W. Huang, W. Z. Chen, and W. C. Cui, "Resolving the shape of a sonoluminescence pulse in sulfuric acid by the use of streak camera," *Journal of the Acoustical Society of America* **125**, 3597-3600 (2009).

13 A. Moshaii, K. Imani, and M. Silatani, "Sonoluminescence radiation from different concentrations of sulfuric acid," *Phys. Rev. E* **80**, 046325 (2009).

14 H. X. Xu, N. C. Eddingsaas, and K. S. Suslick, "Spatial Separation of Cavitating Bubble Populations: The Nanodroplet Injection Model," *J. Am. Chem. Soc.* **131**, 6060-6061 (2009).

15 D. Sunartio, K. Yasui, T. Tuziuti, T. Kozuka, Y. Iida, M. Ashokkumar, and F. Grieser, "Correlation between Na* emission and "Chemically active" acoustic cavitation bubbles," *ChemPhysChem* **8**, 2331-2335 (2007).

16 C. Sehgal, R. P. Steer, R. G. Sutherland, and R. E. Verrall, "Sonoluminescence of argon saturated alkali - metal salt-solutions as a probe of acoustic cavitation," *J. Chem. Phys.* **70**, 2242-2248 (1979).

17 E. B. Flint and K. S. Suslick, "Sonoluminescence from alkali-metal salt solutions," *J. Phys. Chem.* **95**, 1484-1488 (1991).

18 T. J. Matula, R. A. Roy, and P. D. Mourad, "Comparison of Multibubble and Single-Bubble Sonoluminescence Spectra," *Phys. Rev. Lett.* **75**, 2602-2605 (1995).

19 M. Wall, M. Ashokkumar, R. Tronson, and F. Grieser, "Multibubble sonoluminescence in aqueous salt solutions," *Ultrason. Sonochem.* **6**, 7-14 (1999).

20 F. Lepoint-Mullie, N. Voglet, T. Lepoint, and R. Avni, "Evidence for the emission of 'alkali-metal-noble-gas' van der Waals molecules from cavitation bubbles," *Ultrason. Sonochem.* **8**, 151-158 (2001).

21 T. Kozuka, S. Hatanaka, T. Tuziuti, K. Yasui, and H. Mitome, "Observation of a sonoluminescing bubble using a stroboscope," *Jpn. J. Appl. Phys.* **39**, 2967-2968 (2000).

22 T. Kozuka, S. Hatanaka, K. Yasui, T. Tuziuti, and H. Mitome, "Simultaneous observation of motion and size of a sonoluminescing bubble," *Jpn. J. Appl. Phys.* **41**, 3248-3249 (2002).

23 Y. Hayashi and P. K. Choi, "Effects of alcohols on multi-bubble sonoluminescence spectra," *Ultrasonics* **44**, e421-e425 (2006).

24 P. K. Choi, S. Abe, and Y. Hayashi, "Sonoluminescence of Na atom from NaCl solutions doped with ethanol," *J. Phys. Chem. B* **112**, 918-922 (2008).

25 S. Abe and P. K. Choi, "Spatiotemporal Separation of Na-Atom Emission from Continuum Emission in Sonoluminescence," *Jpn. J. Appl. Phys.* **48** (2009).

26 S. Hatanaka, K. Yasui, T. Tuziuti, T. Kozuka, and H. Mitome, "Quenching mechanism of multibubble sonoluminescence at excessive sound pressure," *Jpn. J. Appl. Phys., Part 1* **40**, 3856-3860 (2001).

27 W. B. McNamara, Y. T. Didenko, and K. S. Suslick, "Sonoluminescence temperatures during multi-bubble cavitation," *Nature* **401**, 772-775 (1999).

28 S. Yi. Chen and M. Takeo, "Broadening and Shift of Spectral Lines Due to the Presence of Foreign Gases," *Rev. Mod. Phys.* **29**, 20-73 (1957).

29 K. S. Suslick, D. A. Hammerton, and R. E. Cline, "The Sonochemical Hot-Spot," *J. Am. Chem. Soc.* **108**, 5641-5642 (1986).